Adsorption (2011) 17: 361–370
DOI 10.1007/s10450-011-9336-4

Adsorptive properties of X zeolites modified by transition metal cation exchange

Souhila Bendenia · Kheira Marouf-Khelifa · Isabelle Batonneau-Gener · Zoubir Derriche · Amine Khelifa

Received: 31 March 2009 / Accepted: 7 February 2011 / Published online: 23 February 2011

Abstract The ionic exchange of the NaX zeolite by Ni^{2+} and Cr^{3+} cations was progressively driven and studied by adsorption of nitrogen and carbon dioxide. For each cation-exchanged X zeolite sample, the development of characteristics such as profile of isotherms, RI criterion, isosteric adsorption heat and microporous volume using both the Dubinin–Radushkevich (DR) equation and the t-plot, was followed through the nitrogen adsorption. Results show that the cationic exchange process, in the case of Cr^{3+} introduced at middle degree, is accompanied by a textural damage for Cr(x)X, in contrast to Ni^{2+}-exchanged X zeolites. This degradation occurs without significant presence of mesopores, because the RI criterion values were found to be much lower than 2.2. The CO_2 adsorption isotherms were measured at intervals of 30 K from 273 K and the equilibrium pressures ranged from 0.5 to 600 Torr. The experimental data were correlated by the Toth model. The associated three adjustable parameters were estimated by non-linear least-squares analysis. The effect of temperature on the model parameters and the Henry's law slope, K_H, represented by the product of Toth parameters, are discussed.

Keywords Zeolite · Ion exchange · Adsorption · Isotherm · N_2 · CO_2

S. Bendenia · A. Khelifa (✉)
Laboratoire de Structure, Elaboration et Applications des Matériaux Moléculaires (S.E.A.2M.), Département de Chimie, Université de Mostaganem, B.P. 981, R.P., Mostaganem 27000, Algeria
e-mail: aminekhelifadz@yahoo.fr

K. Marouf-Khelifa
Laboratoire S.T.E.V.A., Département de Chimie, Université de Mostaganem, Mostaganem, Algeria

I. Batonneau-Gener
Laboratoire LACCO, UMR 6503, 40 avenue du Recteur Pineau, 86022 Poitiers, France

Z. Derriche
Laboratoire de Physico-Chimie des Matériaux, Département de Chimie, USTO-MB, Oran, Algeria

1 Introduction

Synthetic zeolites are an important class of solid materials that are used extensively in many fields, such as gas storage, catalysis and ion-exchange (Breck 1974; Dyer 1988). Owing to their stable crystal structure, large pore volume and high cation content, type X zeolites are extensively used in adsorption and separation processes (Ruthven 1984). The carbon dioxide and nitrogen adsorption methods are commonly used to quantify the parameters associated to these processes. Both N_2 and CO_2 possess quadrupole moments which may be expected to interact strongly with extra-framework cations. These cations are known to occupy three main sites within the cages: sites I in hexagonal prisms, sites I′ in the sodalite cage near the hexagonal prisms, sites II in the centre of the six-membered rings of the supercage, sites II′ in the sodalite cage near a six-membered ring and sites III at the entrance of the supercage (Mortier 1982). They can participate to ion-exchange processes with other type of cations from primarily aqueous solutions.

N_2, CO_2 and other guest molecules adsorption onto cation-exchanged X zeolites have been extensively studied to determine the effect of ion type on the adsorption equilibrium and energetics (Jayaraman et al. 2002; Siporin et al. 2003; Maurin et al. 2005; Manjare and Ghoshal 2006; Walton et al. 2006; Derkowski et al. 2007; Díaz et al. 2008). Despite evidence in the literature of increased interest in zeolites containing polyvalent cations of transition metals, no

adsorption study has yet been published on X zeolite exchanged with Ni^{2+} and Cr^{3+} ions at different percentages of exchange. On the other hand, the introduction of Ni^{2+} and Cr^{3+} cations into zeolites may lead to interesting catalytic properties. For instance, the production of fuel and lubricants is obtained by oligomerization of olefins on nickel and chromium containing MCM-41 (Pelrine et al. 1992, 1993). The fact that the adsorptive properties are affected by the percentage and the distribution of cations within the zeolitic lattice obviously implies that it is the same for the catalytic properties.

NaX was progressively modified by Ni^{2+} and Cr^{3+} ions and adsorption characteristics were followed simultaneously. The textural properties were investigated by the nitrogen adsorption. The results were discussed through the assessment of microporosity using various methods including BET equation, t-plot, Dubinin–Radushkevich method, RI criterion and thermodynamic data such as the isosteric heat. The adsorption equilibria of CO_2 onto X zeolites modified by Ni^{2+} and Cr^{3+} cations at different rates of exchange were measured by a static gravimetric method. The experimental data obtained at various temperatures were correlated with the Toth model. The effect of temperature on the model parameters and the Henry's law slope, K_H, represented by the product of Toth parameters, are discussed.

2 Experimental part

2.1 Materials

The NaX zeolite (Si/Al = 1.21, unit cell formula $Na_{87}(AlO_2)_{87}(SiO_2)_{105}\ nH_2O$) was supplied by CECA Co. Ionic exchange was carried out at room temperature by stirring 2 g of parent zeolite in 100 ml of aqueous solution containing the metal nitrate for 24 h. The sample was washed until free of nitrate and dried overnight at 353 K. 0.1 g of each ion-exchanged sample was dissolved using HF–H_3BO_3 (Bernas 1968) and analyzed by means of a Perkin–Elmer 2380 atomic absorption spectrophotometer. A sample M(x)X indicates a zeolite derived from the X sample, and exchanged with Ni^{2+} or Cr^{3+} ions. The number, x, in the sample name indicates the percentage of ion-exchange (e.g. Ni(61)X means 61% of Na^+ ions are replaced with Ni^{2+} cations). The operating conditions are summarised in Table 1.

2.2 Procedure

The nitrogen adsorption isotherms were measured at 77 K via an ASAP 2010 instrument (Micromeritics, Norcross, GA, USA), using helium and nitrogen of 99.99% purity as supplied by Air Liquide. The samples were first outgassed at 573 K for at least 4 h under vacuum. The texture was investigated across the parameters such as the BET surface area, the RI criterion, the micropore volume and external surface area through the Lippens–de Boer and Dubinin–Radushkevich methods (Gregg and Sing 1982).

The carbon dioxide adsorption isotherms were measured thermogravimetrically using the Ugine–Eyraud, B. 70, Setaram, thermobalance. A detailed description of the device is given in a previous work (Khelifa et al. 1999a). About 300 mg of the zeolite sample was preliminarily activated at 673 K in a secondary dynamic vacuum using an oil diffusion pump. The temperature was raised at a rate of 40°/h to 673 K and maintained at that temperature for a further 12 h. High purity (>99.9%) carbon dioxide was obtained from Sidal, France.

For the collection of adsorption data, the doses of adsorbate were sequentially introduced. The time for the establishment of adsorption equilibrium was 3 h for the first points of isotherm, while 20 min was sufficient at higher pressures. The estimated error in measurement for an adsorption of 10 mg of adsorbate was 1%. Desorption isotherms were measured. The results show that the adsorption and desorption are carried out without a hysteresis loop.

Table 1 Experimental conditions during the preparation of Ni(x)X and Cr(x)X

Zeolite	Initial concentration of [Ni^{2+}] or [Cr^{3+}] (mol l^{-1})	Ni^{2+} or Cr^{3+} cations/ unit cell	Unit cells/g $\times 10^{-19}$	Molecules/ pseudo unit cell	Equilibrium pH
NaX	0	0.0	4.48	13.43	–
Ni(40)X	0.05	17.4	4.41	13.65	7.56
Ni(61)X	0.1	26.5	4.37	13.77	6.59
Ni(72)X	0.5	31.3	4.35	13.83	6.19
Cr(19)X	0.001	5.5	4.51	13.34	8.35
Cr(32)X	0.005	9.3	4.54	13.28	7.08
Cr(39)X	0.01	11.3	4.55	13.24	6.50
Cr(45)X	0.1	13.1	4.56	13.21	3.68

2.3 Theoretical considerations

2.3.1 *Calculation of the RI criterion (Ginoux and Bonnetain 1991)*

The tangent at the inflection point of the isotherm is drawn, and its intercepts with the vertical axes at relatives pressures $p/p_0 = 0$ and 1 are evaluated. If the ratio of these intercepts (referred to as RI) is lower than 2.2, the BET equation cannot represent the isotherm and microporosity is likely to be involved. For RI greater than 2.2, the BET equation generally represents fairly well the experimental isotherm, suggesting that microporosity is negligible or absent.

2.3.2 *Method of Lippens and de Boer (1965)*

This method allows the measurement of the micropore volume and external surface area. It is based on the comparison of the shape of a given isotherm with that of a standard isotherm of a nonporous reference solid. It is founded on the concept of the statistical thickness (t) which is calculated, for nitrogen at 77 K, from the ratio $t = 3.54V/V_{\mathrm{m}}$, V_{m} being the monolayer capacity, determined from the BET plots.

For a microporous solid, the t-plot, i.e. the curve of the amount adsorbed plotted against t, presents the form of curve. The slope of the linear branch of this curve gives the external surface area, S_{ext}, whereas the intercept on the y-axis of the extrapolated linear part leads to the micropore volume, $W_{0,t}$.

2.3.3 *Method of Dubinin and Radushkevich (1947)*

This method is based on a process of volume filling of the micropores and is expressed by the relation:

$$\ln V = \ln V_0 - \left(\frac{RT}{\beta E_0}\right)^2 \ln^2\left(\frac{p_0}{p}\right) \tag{1}$$

where V and V_0 are the nitrogen adsorption volume at pressure p and saturated vapour pressure p_0, respectively, β is an affinity coefficient, E_0 is the characteristic adsorption heat and T is the liquid nitrogen temperature ($T = 77$ K).

According to (1), the DR plot of $\ln V$ against $\ln^2(\frac{p_0}{p})$ should be a straight line having an intercept equal to V_0 which converted to a liquid volume may be taken as equal to the micropore volume, $W_{0,\mathrm{DR}}$. From βE_0, the isosteric adsorption heat at coverage θ of $1/e$, $q_{\mathrm{st}}^{\theta=1/e}$, can be obtained by the equation:

$$q_{\mathrm{st}}^{\theta=1/e} = \beta E_0 + \Delta H_L \tag{2}$$

where ΔH_L is the liquefaction enthalpy of nitrogen ($\Delta H_L = 5.58$ kJ mol^{-1} at 77 K).

2.3.4 *Toth's isotherm*

The Toth isotherm is frequently used to correlate the adsorption equilibrium data of many solids, such as zeolites. It is a three-parameter model usually written in the form:

$$n = \frac{n_s K P}{[1 + (K P)^m]^{1/m}} \tag{3}$$

where P is the equilibrium pressure; n_s is the monolayer capacity; m is a parameter describing energetic heterogeneity of the adsorbent surface; and K is related to the Henry's law slope.

The parameters obtained from the best fit to the experimental data have been determined by nonlinear regression, with the average relative errors, E_{rm}, calculated by the relation:

$$E_{\mathrm{rm}}(\%) = \frac{100}{N_{\mathrm{exp}}} \sum_{0}^{N_{\mathrm{exp}}} \left| \frac{n_{\mathrm{exp}} - n}{n_{\mathrm{exp}}} \right| \tag{4}$$

where n_{exp} is the experimental amount of adsorbate, n that calculated with the model, and N_{exp} the number of experimental data.

3 Results and discussion

3.1 Nitrogen adsorption

The nitrogen adsorption isotherms, for each of the cation exchanged forms listed in Table 1, are shown in Fig. 1. The observation of the curves reveals that the adsorption isotherms are of type I, indicating primarily a volume filling of micropores. The filling of micropores is completed for approximately $p/p_0 = 0.3$. Beyond, adsorption is carried out outside micropores. For a majority of the samples, the quantity adsorbed between $p/p_0 = 0.3$ and 0.94 is relatively small, around 10%, compared to that adsorbed within the micropores (Table 2). Knowing that the latter are saturated from the lowest relative pressures, the difference in adsorbed quantity, between $p/p_0 = 0.3$ and 0.94, could be ascribed to adsorption on the external surface of zeolitic crystallites. For Cr(45)X, the adsorption capacity outside the micropores is much more significant, namely 36.1%. The causes of this phenomenon will be discussed later.

The RI values for the nitrogen adsorption are presented in Table 2. The values vary between 1.04 and 1.67 suggesting that the mesoporosity is negligible or absent whatever the sample considered. The closer the RI value to 1, the lower adsorbed amount outside micropores should be. RI is somewhat higher for Cr(45)X, namely 1.67. Amari et al. (1994) reported that RI changes either when the external surface or the microporous volume varies.

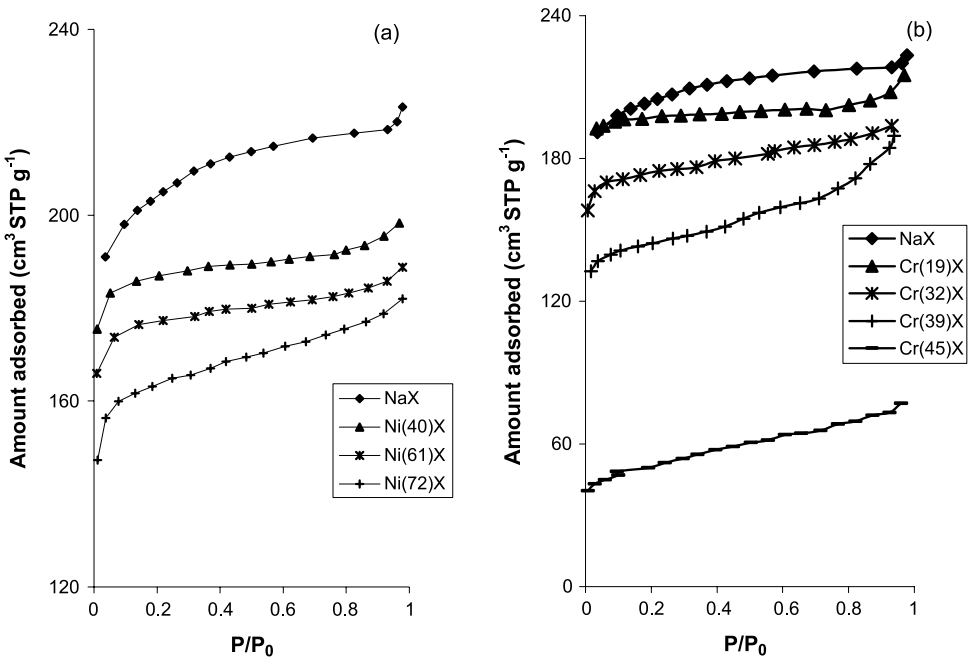

Fig. 1 Isotherms of N_2 adsorption on (**a**) Ni(x)X; (**b**) Cr(x)X

Table 2 N_2 adsorption characteristics of ion-exchanged X zeolites

Zeolite	Amount adsorbed ($Q_{0.3}$) at $p/p_0 = 0.3$[a] (cm^3 STP g^{-1})	Amount adsorbed ($Q_{0.94}$) at $p/p_0 = 0.94$[a] (cm^3 STP g^{-1})	Adsorption outside micropores $[Q_{0.94} - Q_{0.3}/Q_{0.3}]\cdot 100$ (%)	RI	$q_{st}^{\theta=1/e}$ (kJ mol^{-1})
NaX	208.7	218.8	4.7	1.06	16.9
Ni(40)X	188.1	196.2	4.3	1.05	16.3
Ni(61)X	178.1	186.2	4.5	1.06	16.6
Ni(72)X	165.5	179.1	8.2	1.12	13.7
Cr(19)X	198.2	209.0	5.4	1.04	17.1
Cr(32)X	175.9	194.4	10.5	1.15	15.1
Cr(39)X	157.0	183.7	17.0	1.28	13.7
Cr(45)X	54.0	73.5	36.1	1.67	11.8

[a] p_0: Saturated vapour pressure of nitrogen at 77 K

Bearing in mind that cations act as adsorption centres, their distribution among non-framework sites determines their adsorptive behaviour. From Table 2, it is seen a decrease in the N_2 uptake with increasing number of M^{n+} ions. Firstly, the free diameter of six-membered oxygen windows controlling access to the sodalite cages and hexagonal prisms is 0.26 nm while the kinetic diameter of the nitrogen molecule is 0.364 nm; consequently N_2 is only adsorbed in the supercages. Secondly, N_2 is a cation-specific adsorbate (Kazansky et al. 2001). From these considerations, the decrease in the N_2 uptake capacity with the degree of Na^+ replacement by Ni^{2+} and Cr^{3+} cations could be thus ascribed to a decrease in cationic density within supercages. In other words, cations Ni^{2+} and Cr^{3+} preferentially occupy inaccessible sites, localised within the sodalite units (I′, II′) and hexagonal prisms (I). Kim et al. (1994) also reported a preferential filling of inaccessible sites by Ce^{3+} and La^{3+} ions inserted into NaX zeolite. Consequently, the capacity of the nitrogen adsorption by the exchanged zeolites can be only less significant, compared to that of the parent zeolite. This is also due to the decrease in the number of extraframework cations, while n monovalent sodium ions are replaced with one M^{n+}. The same phenomenon was observed, in the case of the N_2 adsorption on Cu(x)X, Zn(x)X and CuZn(x)X (Hammoudi et al. 2008), C_3H_6 on Cu(x)X (Khelifa et al. 1999b) and CO_2 on Cu(x)X and Zn(x)X (Khelifa et al. 2001a).

In order to evaluate the strength of adsorbate/adsorbent interactions, the isosteric adsorption heats were calculated and presented in Table 2. For NaX, the value of $q_{st}^{\theta=1/e}$ is 16.9 kJ mol^{-1}. The enthalpy of nitrogen adsorption on NaX reported in the literature is around 20 kJ mol^{-1} (Maurin et

Table 3 Textural properties of ion-exchanged X zeolites

Zeolite	BET surface area, S_{BET} ($m^2\ g^{-1}$)	Micropore volume, $W_{0,DR}$ ($cm^3\ g^{-1}$)	Micropore volume, $W_{0,t}$ ($cm^3\ g^{-1}$)	External surface area, S_{ext} ($m^2\ g^{-1}$)
NaX	622.1	0.315	0.327	2.3
Ni(40)X	582.7	0.289	0.279	2.1
Ni(61)X	537.1	0.274	0.266	2.5
Ni(72)X	498.2	0.254	0.243	3.8
Cr(19)X	589.2	0.304	0.293	2.2
Cr(32)X	528.6	0.269	0.246	1.9
Cr(39)X	451.8	0.224	0.211	2.5
Cr(45)X	161.7	0.077	0.065	4.5

al. 2005; Dunne et al. 1996). Our value is not underestimated because theirs was given at zero coverage ($\theta = 0$) which is generally higher than that found at $\theta = 1/e$. Transition metal complexes are reported to interact with N_2 through end-on coordination (M–N≡N) (Nakamoto 1997). The adsorption of nitrogen on the cobalt-exchanged zeolite X with different cobalt content was investigated (Sebastian et al. 2005). The stronger interactions of the nitrogen molecules were explained in terms of the π-complexation between nitrogen molecules and extraframework cobalt cations of the zeolites. By Microcalorimetry measurements, the adsorption of nitrogen by divalent (Ca^{2+}, Sr^{2+}, Ba^{2+}) ion exchanged X-faujasites was interpreted through a combination of both electrostatic and polarization contributions (Maurin et al. 2005). By DRIFT spectroscopy, it has been reported that the nitrogen adsorption by NaLSX and LiLSX zeolites, a FAU-framework with Si/Al = 1, leads to polarization of N_2 molecules, which results from their adsorption on Na^+ or Li^+ cations (Kazansky et al. 2001).

As the degree of exchange increases the heat of adsorption decreases for Cr(x)X–N_2 systems. This evolution has also been reported in the case of the N_2 adsorption on Cu(x)X (Hammoudi et al. 2008). The continuous decrease in isosteric heat with the introduction of Cr^{3+} could be ascribed to a progressive weakening of electrostatic fields present within zeolitic cavities.

The strength of adsorbate/adsorbent interactions cannot be explained in terms of the π-complexation between nitrogen molecules and extraframework nickel and chromium cations, because the $q_{st}^{\theta=1/e}$ values are not very high. The involved mechanism could be due to a combination of both electrostatic and polarization contributions, which result from the nitrogen adsorption on Na^+, Ni^{2+} and Cr^{3+} cations.

The micropore volumes, $W_{0,DR}$, were determined by N_2 adsorption using the Dubinin–Radushkevich (DR) equation. To determine the external surface areas, S_{ext}, the isotherms were analysed by the t-plot through the Lippens and de Boer method which also makes it possible to obtain the volume of micropores, $W_{0,t}$. The specific surface areas were estimated by the BET equation. All derived data are listed in Table 3.

The value of $W_{0,DR}$ found for NaX, 0.315 $cm^3\ g^{-1}$, is in good agreement with that reported by Maurin et al. (2005), namely 0.304 $cm^3\ g^{-1}$, whereas values of 0.27 and 0.35 $cm^3\ g^{-1}$ were reported by Du and Wu (2007) and Joshi et al. (2001), respectively. Beutekamp and Harting (2002) reported a micropore volume of 0.21 $cm^3\ g^{-1}$ for 13X zeolite but for a specific area, S_{BET}, equal to 383 $m^2\ g^{-1}$ while the S_{BET} value of our NaX, supplied by CECA Co, is 622 $m^2\ g^{-1}$.

The values of micropore volume, $W_{0,DR}$, for the exchanged zeolites, are slightly higher than that of $W_{0,t}$ (Table 3), in spite of the low values of the external surface area obtained in this study. Remy and Poncelet (1995) suggested that the DR equation overestimated $W_{0,DR}$, with respect to $W_{0,t}$, when a solid presents an important external surface. Our value of S_{ext} for NaX, 2.3 $m^2\ g^{-1}$, is close to that found by Ginoux (1983), namely 2 $m^2\ g^{-1}$ and by Amari et al. (1994) for NaA, i.e. 3.7 $m^2\ g^{-1}$.

The evolution of micropore volume of Ni(x)X and Cr(x)X with the cation exchange level, obtained from the Lippens-de Boer method is illustrated in Fig. 2. The values of micropore volume slightly decreases for Ni(x)X, the main cause being the decrease in cationic density within supercages and a preferential filling of inaccessible sites within the sodalite cage (sites I′ and II′) and/or the hexagonal prism (sites I), when two monovalent sodium ions are replaced with one Ni^{2+} ion, as mentioned above. For Cr(x)X, $W_{0,t}$ markedly decreases, in particular for Cr(45)X, namely at middle exchange degree, so that the depopulation of the cationic sites distributed within the supercages cannot be invoked. It is interesting to note that the external surface of Cr(45)X is twice larger than that of NaX (Table 3), whereas its adsorption capacity outside the micropores is much more significant, i.e. 36.1% (Table 2). These features indicate a clear textural damage with the introduction of Cr^{3+} cations in the zeolitic framework of X zeolites, at least at percentage of exchange about 50%. This is also supported by the

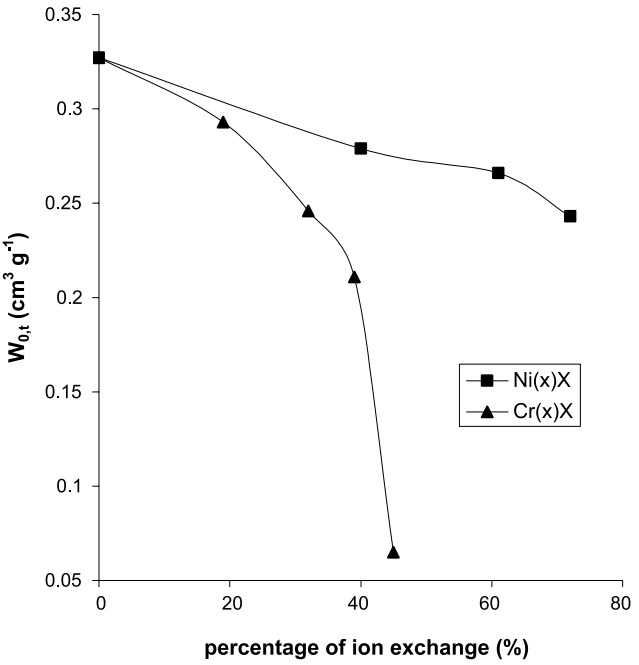

Fig. 2 Evolution of micropore volume, $W_{0,t}$, versus percentage of ion-exchange

sharp decrease of crystallinity percentage of Cr(45)X, i.e. 34% (Khelifa et al. 2006).

The sensitivity of the crystalline structure of Cr(45)X could be explained in terms of structural deformation. Adsorbate molecules can interact with the zeolite surface through lattice oxygen atoms, accessible extraframework cations, and Al and Si atoms. Knowing that Al and Si atoms present at the centre of tetrahedra are not directly exposed to the adsorbate molecules, the principal interactions of the latter with the zeolite surface are with lattice oxygen atoms and extraframework cations (Cohen de Lara and Delaval 1978), such as chromium. The deformation would thus consist of a change of the supercage geometry which would influence the adsorption characteristics. In other words, Cr^{3+} severely distorts or destroys the zeolitic crystal at middle exchange levels. Pansini et al. (1991) attribute this relative deterioration to the strong affinity of Cr^{3+} ions for oxygens constituting the zeolitic lattice. This effect leads to the distortion of six oxygens surrounding the Cr^{3+} cations located in the sites of compensation of negative charges.

3.2 Carbon dioxide adsorption

Families of isotherms for carbon dioxide adsorption on cation-exchanged zeolites are presented in Fig. 3. The adsorbed amount is expressed in molecules per unit cell, since the number of unit cells per gram of dehydrated zeolites varies. For this reason, we reported in Table 1 the conversion factors in unit cells/g and molecules/unit cell. The latter are relative to 1 mmol/g. The isotherms were measured at intervals of 30 K and the equilibrium pressures ranged from 0.5 to 600 Torr. NaX adsorbs 5.04 mmol/g at 303 K and 352 Torr, which is in agreement with the reported data (Dunne et al. 1996) under similar conditions.

The IUPAC classification of gas–solid adsorption isotherms covers the behaviour of a great number of adsorption systems. Thus according to the IUPAC recommendations (1994), the first step is to identify the isotherm type and hence the nature of the adsorption process. The experimental isotherms obtained are of type I from this classification, at least at low temperature. Type I isotherms approach a limiting value at high pressures and usually are used to describe adsorption on microporous solids such as zeolites. This limit is justified by noting that the volume of the adsorbed phase is limited by the volume of the microporosity at which adsorption is done.

Fitting of adsorption isotherm equations to experimental data is an important aspect of data analysis. The structural regularity of zeolite lattices and the existence of well-defined cavities within which the adsorbate molecules are lodged suggest that it should be possible to use various isotherm equations. In this connection, the thermodynamic models, such as those of Langmuir, Fowler, and Volmer ... are selected because they often describe the adsorption of gas on zeolites. In a previous work, these models were used to describe the experimental isotherms of CO_2 adsorption onto Ni(x)X and Cr(x)X (Khelifa et al. 2004). The best fit was obtained with the Sips equation. The average relative errors relating to this model are given in Table 4.

All the above mentioned models use two adjustable parameters which were estimated by linear regression analysis. In this study, the Toth model is used for the mathematical description of the adsorption equilibrium of carbon dioxide onto Ni(x)X and Cr(x)X (Fig. 3). This isotherm equation includes three adjustable parameters and cannot be fitted to the experimental data by linear regression. In this case, it is necessary to apply nonlinear least-squares (NLLS) analysis. Related parameters, namely n_s, m and K, were calculated and listed in Table 4. The determination coefficients and the average relative errors were also calculated as an indicator of fitting of the experimental data to the model proposed. On the basis of the average relative error values, the Toth equation provides a better fit of the adsorption data than that of Sips. For the latter, E_{rm} values higher than 9% were obtained, while for that of Toth, the E_{rm} values do not exceed 6%.

In general, it can be observed that the monolayer capacity, n_s, decreases with increasing temperature. The decrease in the equilibrium adsorption capacity with temperature also indicates that a low temperature favours carbon dioxide removal by adsorption onto X zeolites. This effect suggests that the mechanism associated involves a physical process. Knowing that CO_2 has a strong quadrupole

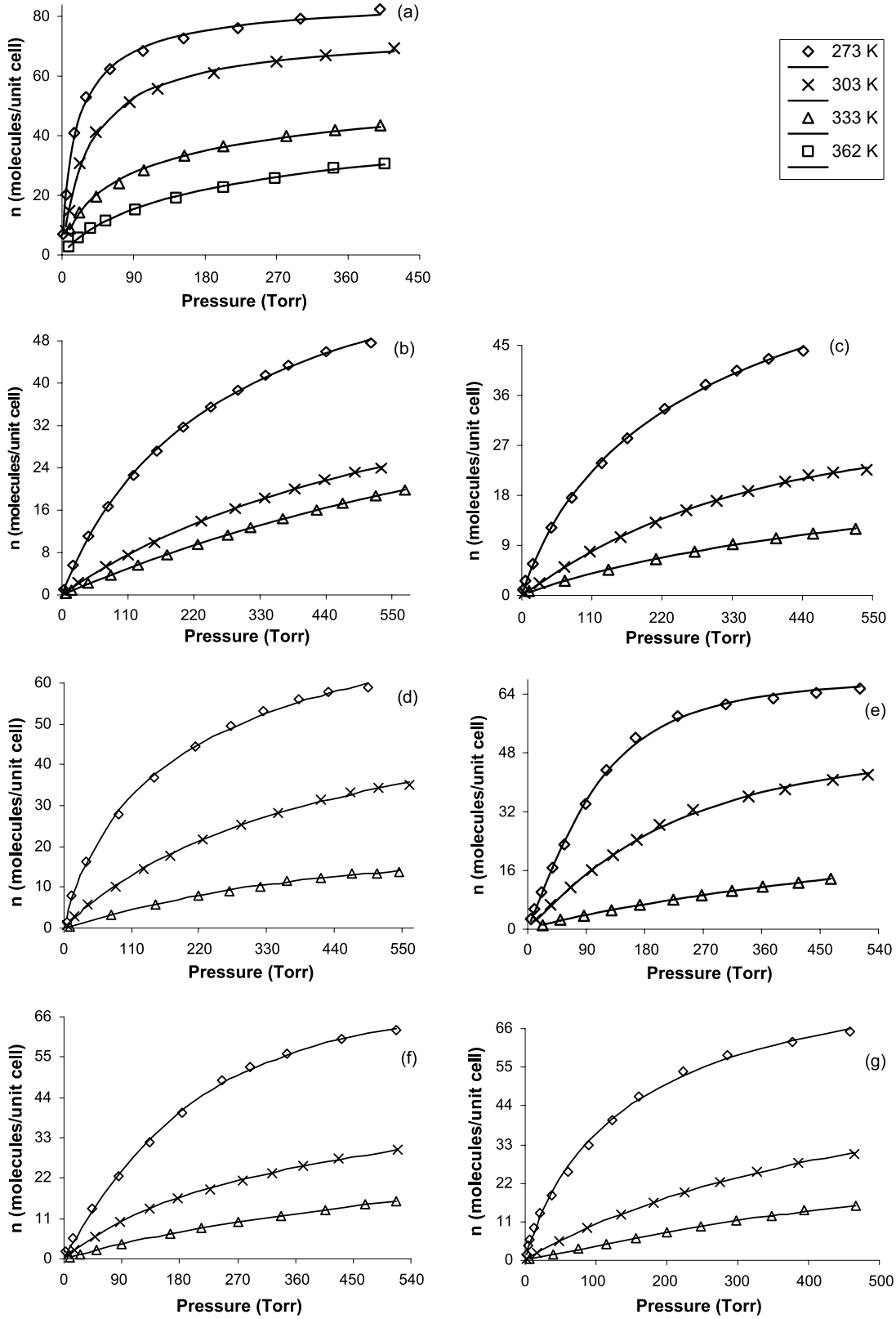

Fig. 3 Isotherms according to experimental data (···) and Toth model (—) for: (**a**) NaX; (**b**) Ni(40)X; (**c**) Ni(61)X; (**d**) Ni(72)X; (**e**) Cr(19)X; (**f**) Cr(32)X; (**g**) Cr(39)X

Table 4 Toth model parameters for CO_2 adsorption isotherms on ion-exchanged X zeolites

Zeolite	T (K)	n_s (molec. unit cell^{-1})	K (Torr^{-1})	m	$n_s * K (K_H)$ (molec unit cell^{-1} Torr^{-1})	Determination coefficient	Average relative error (%)	Average relative error (%)[a]
NaX	273	87.7	0.078	0.781	6.8406	0.998	2.8	4.3
NaX	303	77.2	0.031	0.872	2.3932	0.997	4.2	6.2
NaX	333	67.6	0.027	0.537	1.8252	0.998	2.0	1.3
NaX	362	61.0	0.007	0.610	0.427	0.998	2.5	3.2
Ni(40)X	273	76.8	0.004	0.918	0.3072	0.999	1.9	4.0
Ni(40)X	303	56.9	0.001	0.991	0.0569	0.999	3.3	6.1
Ni(40)X	333	50.0	0.001	1.248	0.05	0.999	2.8	9.2
Ni(61)X	273	81.9	0.005	0.759	0.4095	0.999	4.8	2.0
Ni(61)X	303	33.7	0.002	1.409	0.0674	0.999	2.0	6.9
Ni(61)X	333	38.3	0.001	0.761	0.0383	0.999	5.1	7.5
Ni(72)X	273	90.1	0.008	0.677	0.7077	0.998	6.0	8.3
Ni(72)X	303	68.2	0.002	0.896	0.1364	0.999	3.9	2.6
Ni(72)X	333	21.2	0.002	1.438	0.0424	0.999	1.8	5.2
Cr(19)X	273	69.3	0.007	1.940	0.4851	0.999	4.5	4.9
Cr(19)X	303	53.7	0.003	1.491	0.1611	0.999	2.7	3.5
Cr(19)X	333	50.4	0.001	0.526	0.0594	0.999	2.0	2.3
Cr(32)X	273	75.3	0.004	1.563	0.3012	0.999	5.9	8.1
Cr(32)X	303	67.0	0.002	0.746	0.134	0.999	1.9	3.6
Cr(32)X	333	62.8	0.001	0.648	0.0828	0.999	1.2	2.3
Cr(39)X	273	95.2	0.008	0.816	0.7616	0.998	5.9	8.4
Cr(39)X	303	67.4	0.002	0.989	0.1348	0.999	2.4	1.6
Cr(39)X	333	21.8	0.002	2.509	0.0436	0.999	3.8	2.3

[a]Average relative error (%) from Sips model (Khelifa et al. 2004)

moment, the adsorption process can be probably explained by ion–quadrupole interactions. The monolayer capacity for each isotherm would be reached at pressures much larger than the pressures examined in this study, so there is some extrapolation of the experimental data involved in obtaining n_s from the Toth model.

The product of Toth parameters, $n_s K$, is the Henry's law slope, K_H. This slope is directly related to the interaction of an adsorbate with the surface. Thus, a higher value of K_H indicates a stronger adsorbate-adsorbent interaction. As seen from Table 4, the $n_s K$ product decreases with increasing temperature whatever the sample considered. This evolution also confirms the physical character of carbon dioxide adsorption onto ion-exchanged X zeolites.

The evolution of the mean value of $n_s K$ parameter of each ion-exchanged X zeolite, as a function of the degree of exchange, is presented in Fig. 4. As seen from this figure, the trend for Cr(x)X is not clear, although Cr(39)X exhibits the largest K_H value. A comparison between the Ni(x)X and Cr(x)X samples shows that the latter evidence stronger CO_2–Cr(x)X interactions than that of CO_2–Ni(x)X, at the same rate of exchange; the K_H value being larger.

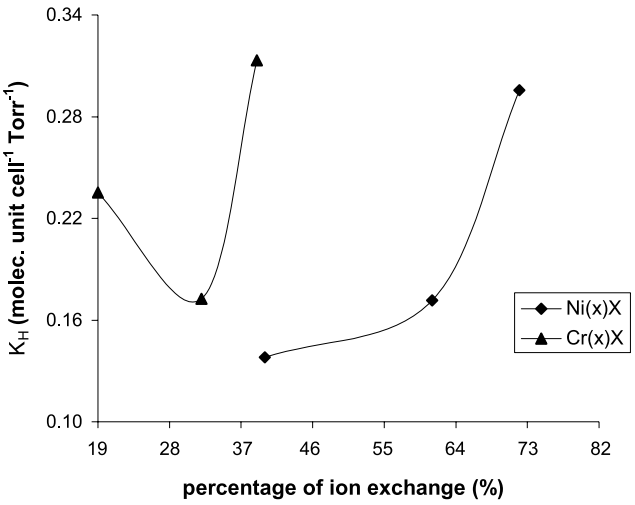

Fig. 4 Evolution of Henry's law slope, K_H, versus rate of exchange.

The interaction of Ni(x)X with CO_2 becomes strong as x increases. Examination of the literature indicates that intermolecular interactions between the adsorbed molecules and

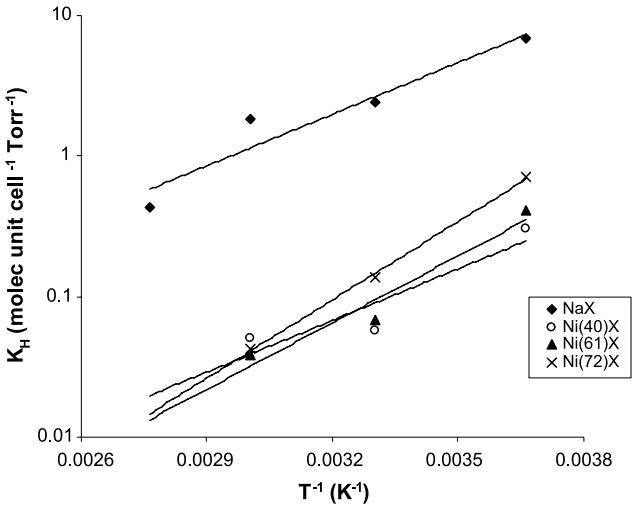

Fig. 5a Van't Hoff plots for CO_2 adsorption on Ni(x)X

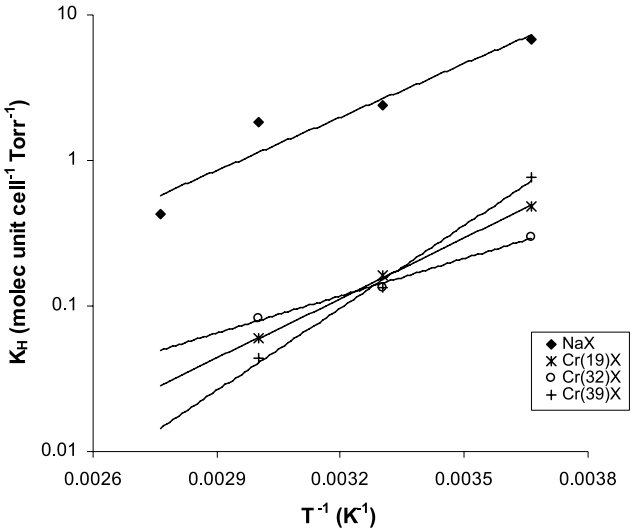

Fig. 5b Van't Hoff plots for CO_2 adsorption on Cr(x)X

M^{2+} cations take place only on zeolites with a sufficiently high degree of exchange (Egerton and Stone 1973). From isosteric heat considerations, it has been shown in an earlier work (Khelifa et al. 2004) that the Ni(61)X and Ni(72)X samples exhibit an energetic heterogeneity generated by the interaction between Ni^{2+} cations present in the supercages and CO_2 molecules. An identical result was found in the case of CO_2 adsorption onto Mg(46)X and Sr(52)X (Khelifa et al. 2001b).

Figures 5a, 5b present the Van't Hoff plots for CO_2 adsorption on Ni(x)X and Cr(x)X which are generally used as a criterion of the adsorption affinity. It should be noted that these values are generated from Toth model. As shown in Fig. 5a, the order of affinities for CO_2, up to 303 K, is Ni(72)X > Ni(61)X > Ni(40)X. The deviation becomes sharper with decreasing temperature. This result is identical with the order of the isosteric heat values, calculated by the Clausius-Clapeyron equation and thoroughly discussed in a previous paper (Khelifa et al. 2004). A reversal in the Henry's constants with reciprocal temperature were observed for Cr(x)X (Fig. 5b). At low temperature, the affinity for CO_2 is dominated by Cr(39)X; from 303 K the highest affinity is manifested by Cr(32)X. This evolution somewhat ambiguous is to be correlated with the strong affinity exerted by Cr^{3+} ions on oxygens constituting the zeolitic lattice, as discussed in a previous section. With the introduction of Cr^{3+}, a progressive weakening of electrostatic fields located within zeolitic cavities of Cr(x)X occurs (Khelifa et al. 2004), so that the behaviour of these solids becomes unpredictable with respect to CO_2 adsorption, with increasing thermal agitation.

4 Conclusions

Replacement of Na^+ by Ni^{2+} or Cr^{3+} in X-type zeolites, profoundly affects the textural and adsorptive properties. The nitrogen adsorption isotherms primarily indicate a volume filling of micropores and no significant presence of mesopores. The values of micropore volume slightly decreases for Ni(x)X, whereas for Cr(x)X, W_0 markedly decreases, in particular at middle exchange degree.

Adsorption isotherms of carbon dioxide were successfully modelled using the Toth equation. This model provided the best fit of the adsorption data, comparatively to models using two adjustable parameters. The Toth isotherm includes three adjustable parameters which were estimated by nonlinear least-squares (NLLS) analysis. The Henry's law slope, K_H, represented by the product of Toth parameters, $n_s K$, is directly related to the interaction of an adsorbate with the surface. The evolution of $n_s K$ parameter confirms the physical character of carbon dioxide adsorption onto ion-exchanged X zeolites. Stronger CO_2–Cr(x)X interactions were obtained comparatively to CO_2–Ni(x)X, at the same level of exchange. Of these, the interaction of Ni(x)X with carbon dioxide becomes strong as the rate of exchange increases.

References

Amari, D., Ginoux, J.L., Bonnetain, L.: Textural damage of cation-exchanged LTA zeolites studied by gas adsorption. Zeolites **14**, 58–64 (1994)

Bernas, B.: A new method for decomposition and comprehensive analysis of silicates by atomic absorption spectrometry. Anal. Chem. **40**, 1682–1686 (1968)

Beutekamp, S., Harting, P.: Experimental determination and analysis of high pressure adsorption data of pure gases and gas mixtures. Adsorption **8**, 255–269 (2002)

Breck, D.W.: Zeolite Molecular Sieves. Wiley-Interscience, New York (1974)

Cohen de Lara, E., Delaval, Y.: Infrared spectra of nitrogen adsorbed in NaA zeolite. Experimental determination of electrostatic field in the cavities from induced band intensity and comparison with theoretical results. J. Chem. Soc. Faraday Trans. II, **74**, 790–797 (1978)

Derkowski, A., Franus, W., Waniak-Nowicka, H., Czímerová, A.: Textural properties vs. CEC and EGME retention of Na–X zeolites prepared from fly ash at room temperature. Int. J. Miner. Process. **82**, 57–68 (2007)

Díaz, E., Muñoz, E., Vega, A., Ordóñez, S.: Enhancement of the CO_2 retention capacity of X zeolites by Na- and Cs-treatments. Chemosphere **70**, 1375–1382 (2008)

Du, X., Wu, E.: Porosity of microporous zeolites A, X and ZSM-5 studied by small angle X-ray scattering and nitrogen adsorption. J. Phys. Chem. Solids **68**, 1692–1699 (2007)

Dubinin, M.M., Radushkevich, L.V.: Proc. Akad. Sci. USSR **55**, 331 (1947)

Dunne, J.A., Rao, M., Sircar, S., Gorte, R.J., Myers, A.L.: Calorimetric heats of adsorption and adsorption isotherms. 2. O_2, N_2, Ar, CO_2, CH_4, C_2H_6, and SF_6 on NaX, H-ZSM-5, and Na-ZSM-5 zeolites. Langmuir **12**, 5896–5904 (1996)

Dyer, A.: An Introduction to Zeolite Molecular Sieves. Wiley-Interscience, New York (1988)

Egerton, T.A., Stone, F.S.: Adsorption of carbon monoxide by zeolite Y exchanged with different cations. J. Chem. Soc. Faraday Trans. I **69**, 22–38 (1973)

Ginoux, J.L.: Thesis, Grenoble (1983)

Ginoux, J.L., Bonnetain, L.: Some problems about gas adsorption isotherm measurements by automated procedures in manometric devices. Stud. Surf. Sci. Catal. **62**, 189–197 (1991)

Gregg, S.J., Sing, K.S.W.: Adsorption, Surface Area and Porosity. Academic Press, London (1982)

Hammoudi, H., Bendenia, S., Marouf-Khelifa, K., Marouf, R., Schott, J., Khelifa, A.: Effect of the binary and ternary exchanges on crystallinity and textural properties of X zeolites. Microporous Mesoporous Mater. **113**, 343–351 (2008)

IUPAC Commission on Colloid and Surface Chemistry Including Catalysis: Pure Appl. Chem. **66**, 1739–1758 (1994)

Jayaraman, A., Yang, R.T., Cho, S.H., Bhat, T.S.G., Choudary, V.N.: Adsorption of nitrogen, oxygen and argon on Na–CeX zeolites. Adsorption **8**, 271–278 (2002)

Joshi, P.N., Joshi, U.D., Kim, T.H., Kim, K.I., Shiralkar, V.P.: The compatibility of compositional and structural features of aluminous large pore zeolites with sorption characteristics. Adsorption **7**, 279–289 (2001)

Kazansky, V.B., Bulow, M., Tichomirova, E.: Specific sorption sites for nitrogen in zeolites NaLSX and LiLSX. Adsorption **7**, 291–299 (2001)

Khelifa, A., Benchehida, L., Benmaamar, Z., Derriche, Z.: Evolution des propriétés structurales et texturales des zéolithes X dans le cas de l'échange binaire et ternaire. Ann. Chim. Sci. Mat. **31**, 11–22 (2006)

Khelifa, A., Benchehida, L., Derriche, Z.: Adsorption of carbon dioxide by X zeolites exchanged with Ni^{2+} and Cr^{3+}: isotherms and isosteric heat. J. Colloid Interface Sci. **278**, 9–17 (2004)

Khelifa, A., Derriche, Z., Bengueddach, A.: Sorption of carbon dioxide by zeolite X exchanged with Zn^{2+} and Cu^{2+}. Microporous Mesoporous Mater. **32**, 199–209 (1999a)

Khelifa, A., Derriche, Z., Bengueddach, A.: Adsorption of propene on NaX zeolite exchanged with Zn^{2+} and Cu^{2+}. Appl. Catal. A, Gen. **178**, 61–68 (1999b)

Khelifa, A., Derriche, Z., Bengueddach, A.: Adsorption of carbon dioxide by X zeolites exchanged with Zn^{2+} and Cu^{2+}: isosteric heat and adsorption isotherms. In: Galarneau, A., DiRenzo, F., Fajula, F., Vedrine, J. (eds.) Stud. Surf. Sci. Catal., vol. 135, p. 225. Elsevier, Amsterdam (2001a)

Khelifa, A., Hasnaoui, A., Derriche, Z., Bengueddach, A.: Adsorption de CO_2 par des zéolithes X échangées par des cations bivalents. Ann. Chim. Sci. Mat. **26**, 55–66 (2001b)

Kim, J.G., Kompany, T., Ryoo, R., Ito, T., Fraissard, J.: ^{129}Xe n.m.r. of Y^{3+}-, La^{3+}-, and Ce^{3+}-exchanged X zeolites. Zeolites **14**, 427–432 (1994)

Lippens, B.C., de Boer, J.H.: Studies on pore systems in catalysts V. The t-Method. J. Catal. **4**, 319–323 (1965)

Manjare, S.D., Ghoshal, A.K.: Adsorption equilibrium studies for ethyl acetate vapor and E-Merck 13X molecular sieve system. Sep. Purif. Technol. **51**, 118–125 (2006)

Maurin, G., Llewellyn, P.L., Poyet, Th., Kuchta, B.: Adsorption of argon and nitrogen in X-faujasites: relationships for understanding the interactions with monovalent and divalent cations. Microporous Mesoporous Mater. **79**, 53–59 (2005)

Mortier, W.J.: Compilation of Extraframework Sites in Zeolites. Butterworth, Guildford (1982)

Nakamoto, K.: Infrared and Raman Spectra of Inorganic and Coordination Compounds. Part B: Applications in Coordination, Organometallic and Bioinorganic Chemistry, 5th edn., pp. 173–177. Wiley-Interscience, New York (1997)

Pansini, M., Colella, C., De Gennaro, M.: Chromium removal from water by ion exchange using zeolite. Desalination **83**, 145–157 (1991)

Pelrine, B.P., Schmidt, K.D., Vartuli, J.C.: US Patent no. 5,105,051 (1992)

Pelrine, B.P., Schmidt, K.D., Vartuli, J.C.: US Patent no. 5,270,273 (1993)

Remy, M.J., Poncelet, G.: A new approach to the determination of the external surface and micropore volume of zeolites from the nitrogen adsorption isotherm at 77 K. J. Phys. Chem. **99**, 773–779 (1995)

Ruthven, D.M.: Principles of Adsorption and Adsorption Processes. Wiley-Interscience, New York (1984)

Sebastian, J., Peter, S.A., Jasra, R.V.: Adsorption of nitrogen, oxygen, and argon in cobalt(II)-exchanged zeolite X. Langmuir **21**, 11220–11225 (2005)

Siporin, S.E., McClaine, B.C., Davis, R.J.: Adsorption of N_2 and CO_2 on zeolite X exchanged with potassium, barium, or lanthanum. Langmuir **19**, 4707–4713 (2003)

Walton, K.S., Abney, M.B., LeVan, M.D.: CO_2 adsorption in Y and X zeolites modified by alkali metal cation exchange. Microporous Mesoporous Mater. **91**, 78–84 (2006)